35th Annual International Conference of the IEEE EMBS
Osaka, Japan, 3 - 7 July, 2013

Nonlinear Coil Sensitivity Estimation for Parallel Magnetic Resonance Imaging using Data-Adaptive Steering Kernel Regression Method*

Sheng Fang and Hua Guo

Abstract—**The parallel magnetic resonance imag**ing (parallel imaging) technique reduces the MR data acquisition time by using multiple receiver coils**. Coil sensitivity estimation is critical for the performance of parallel imaging reconstruction. Currently, most coil sensitivity estimation methods are based on linear interpolation techniques. Such methods may result in Gibbs-ringing artifact or resolution loss, when the resolution of coil sensitivity data is limited. To solve the problem, we proposed a nonlinear coil sensitivity estimation method based on steering kernel regression, which performs a local gradient guided interpolation to the coil sensitivity. The *in vivo* experimental results demonstrate that this method can effectively suppress Gibbs ringing artifact in coil sensitivity and reduces both noise and residual aliasing artifact level in SENSE reconstruction.**

I. Introduction

Parallel Magnetic Resonance Imaging (parallel imaging) uses multiple receiver coils to simultaneously acquire MR signals with sub-Nyquist sampling rate. With the spatial information provided by the sensitivity distribution of receiver coils, these signals can be restored into a un-aliased image via proper reconstruction algorithms. Previously proposed algorithms include k-space based methods such as SMASH[1], GRAPPA[2] PARS[3] and KSPA[4], image-domain based methods such as SENSE[5] and PILS[6], and hybrid methods such as SPACE RIP[7].

Among these methods, SENSE (sensitivity encoding) has the benefit of mathematical accuracy. However, it is sensitive to the accuracy of receiver coil sensitivity estimate since it explicitly requires the knowledge of receiver coil sensitivity to unfold the aliased data set [5]. The data for coil sensitivity calibration can be obtained by using either an additional low resolution scan[5, 8, 9] or the autocalibrated signal (ACS) based on a self-calibrated data acquisition scheme [10-13]. For both strategies, the natural way for increasing the sensitivity accuracy is to increase the data resolution. However, this is usually prohibited by the limited scan time. With limited calibration data resolution, coil estimation method is probably the most important way of improving the coil sensitivity accuracy. Currently, most estimation methods utilize linear interpolation to obtain a full-size coil sensitivity map. Typically, the low resolution data were first low-pass filtered, zero-pad it to the size of the desired image, and Fourier transformed back to image space [10]. Although simple, this linear interpolation method is essentially un-adaptive and has an intrinsic trade-off between resolution and Gibbs-ringing artifact, which may lose spatial information in the calibration data and result in worse geometry factor [5].

To this problem, a new nonlinear estimation algorithm based on nonlinear steering kernel regression method was proposed for more accurate coil sensitivity estimation. The proposed method first estimates a low resolution sensitivity map and then adaptively interpolates it into the size of the desired image using steering kernel regression method [14] that performs a local and adaptive data fitting. The method was experimented using *in vivo* brain image. The results demonstrate that the method can effectively suppress the Gibbs-ringing without sacrifice the resolution. The corresponding SENSE reconstruction also exhibits lower noise level.

II. Sense and Standard Coil Estimate Method

A. The standard SENSE model

The magnetic resonance signal data acquired by a receiver coil can be formulated as:

$$s_j(\vec{k}) = \int \rho(\vec{r}) C_j(\vec{r}) e^{-i\vec{k}\bullet\vec{r}} \bullet d\vec{r}, \qquad (1)$$

where $\rho(\vec{r})$ is the spin density of the desired object at spatial position $\vec{r}$, $C_j(\vec{r})$ is the coil sensitivity of *j*-th coil. $s_j(\vec{k})$ is the signal at k-space position $\vec{k}$ which is acquired by the *j*-th receiver coil. The discretization of (1) leads to the following the linear equation:

$$\vec{d} = \mathbf{E}\vec{m}, \qquad (2)$$

where $\vec{d}$ is a vector formed by the k-space data acquired from all the coils and $\vec{m}$ is the unknown vector formed by spin density of the desired object. The system matrix **E** consists of the product of Fourier coefficient $e^{-i\vec{k}\bullet\vec{r}}$ and the coil sensitivity $C_j(\vec{r})$.

In order to reduce the acquisition time, the parallel imaging technique simultaneously acquires the data below

*Resrach supported by national natural science foundation of China. Grant No. 81101030.

Sheng Fang is with the Institute of Nuclear and New Energy Technology, Tsinghua University, 100084, Beijing, China (phone: 86-10-62782419; fax: 86-10-62792474; e-mail: fangsheng@tsinghua.edu.cn).

Kui Ying is with the Department of Engineering Physics, Tsinghua University, 100084, Beijing, China (e-mail: yingkui@tsinghua.edu.cn).

Hua Guo is with the Center for Biomedical Imaging Research, Department of Biomedical Engineering, Tsinghua University, 100084, Beijing, China (e-mail: huaguo@tsinghua.edu.cn).

the Nyquist sampling rate using multiple coils. With the spatial information contained in the coil sensitivity, the desired image $\vec{m}$ can be reconstructed by inversing the system matrix **E** in (2). The corresponding least square solution can be written as:

$$\vec{m} = (\mathbf{E}^H \boldsymbol{\Psi}^{-1} \mathbf{E})^{-1} \mathbf{E}^H \boldsymbol{\Psi}^{-1} \vec{d} \tag{3}$$

where H indicates transposed complex conjugate and $\boldsymbol{\Psi}$ is the noise covariance matrix [5]. Equation (3) is the solution of the standard SENSE which takes the sampling noise into consideration. However, since the system matrix **E** is ill-conditioned, even small noise in the data can be significantly amplified by the matrix inversion procedure in (3). Therefore, regularization is needed to stabilize the solution.

B. Standard linear estimation algorithm

The scheme of standard coil sensitivity estimate algorithm was shown in Fig.1. Since the zero-padding operation in the third step introduces significant Gibbs ringing, a linear low pass filtering is needed. Due to the intrinsic trade-off between resolution and Gibbs ringing in Fourier extrapolation methods, the extrapolated image can either have residual Gibbs ringing or reduced resolution. In both cases, the original spatial intensity distribution can be twisted.

Since the polynomial fit has the property that the fitting result exactly goes through the given data points, such error cannot be reduced in the final step and can remain in the estimated coil sensitivity maps.

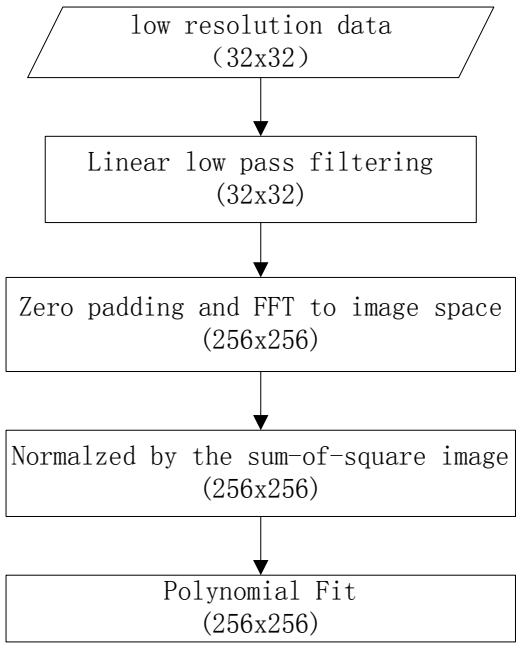

Figure 1. Flow chart of the standard coil sensitivity estimation algorithm. The number in the parenthesis indicates the typical matrix size of the intermediate result at each steps

III. THE PROPOSED NONLINEAR METHOD

A. Steering kernel regression

Nonlinear interpolation methods have been proved to be effective in upscaling (zooming) images with better preserved edges and reduced Gibbs ringing[14-17]. Of all the methods, the steering kernel regression method was chosen for coil sensitivity estimation, because it can automatically adapt itself to local properties of data set. Steering kernel regression can be formulated as a data-adaptive generalization of classical data fitting methods such as the polynomial fitting with spatial adaptive data selection [14].

Following the framework of non-parametric fitting problem, steering kernel regression can be modeled as[14]:

$$y_i(\vec{r}) = k(\vec{r}_i) + \sigma_i(\vec{r}), \quad i = 1, 2, \ldots, P \tag{4}$$

where $y_i(\vec{r})$ is the pixel intensity of acquired single coil sensitivity at spatial position $\vec{r}$, $k(\bullet)$ is the regression function to be estimated; P is the total number of pixels that is involved in the regression function. $\sigma_i(\vec{r})$ is the i.i.d noise.

Using Taylor expansion, the regression function can be approximated as:

$$\begin{aligned} z(\vec{r}_i) &\approx z(\vec{r}) + \nabla z(\vec{r}_i)(\vec{r}_i - \vec{r}) + \frac{1}{2}(\vec{r}_i - \vec{r})^T \mathbf{H}(z)(\vec{r}_i - \vec{r}) + \ldots \\ &= \beta_0 + \beta_1^T (\vec{r}_i - \vec{r}) + \beta_2^T (\vec{r}_i - \vec{r})(\vec{r}_i - \vec{r})^T + \ldots \end{aligned} \tag{5}$$

where $\mathbf{H}(z)$ is the Hessian matrix. For a second-order fitting problem, the kernel regression method finds the most appropriate regression function by solving the following weighted least square minimization:

$$\min_{\{\beta_n\}_{n=0}^2} \sum_{i=1}^{P} [y_i - \beta_0 - \beta_1^T (\vec{r}_i - \vec{r}) - \beta_2^T (\vec{r}_i - \vec{r})(\vec{r}_i - \vec{r})^T]^2 K(\vec{r}_i - \vec{r}) \tag{6}$$

where $K(\vec{r}_i - \vec{r})$ is the regression kernel that can automatically adapts to local image features. And the zero-order Taylor coefficient β_0 is the desired image to be estimated.

B. Steering kernel

Unlike traditional kernel regression that uses a fixed kernel $K(\vec{r}_i - \vec{r})$, steering kernel regression uses an data adaptive kernel based on the covariance of image gradients between pixels involved in the kernel[14]:

$$K(\vec{r}_i - \vec{r}) = \frac{\sqrt{\det(\mathbf{C}_i)}}{2\pi h^2} \exp\left\{ -\frac{(\vec{r}_i - \vec{r})^T \mathbf{C}_i (\vec{r}_i - \vec{r})}{2h^2} \right\} \tag{7}$$

where $\mathbf{C_i}$ is the covariance matrix of spatial gradient vectors of pixels in a neighborhood window centered at position $\vec{r}$, and h is the thresholding parameter that depends on the noise level. The covariance matrix $\mathbf{C_i}$ changes the isotropic Gaussian kernel into an anisotropic kernel that flexibly describes local image gradient distribution. Therefore, the kernel regression can automatically adapt to local image structures.

C. *Nonlinear coil sensitivity estimation using steering kernel regression*

Using steering kernel regression method, the proposed nonlinear coil sensitivity process can be expressed by the following flow chart.

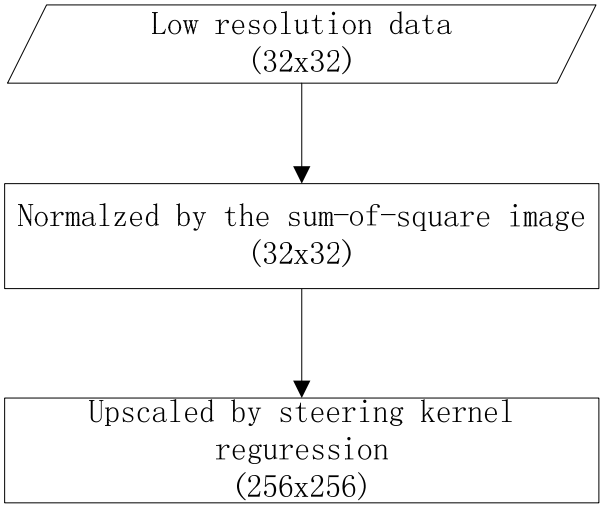

Figure 2. Flow chart of the proposed nonlinear coil sensitivity estimation method

Low resolution coil sensitivity was directly calculated using the acquired data by normalizing each coil images by the sum-of-squares image. Since no interpolation or filtering is performed, no additional error is introduced to the resultant low resolution coil sensitivity. At the last step, the low resolution coil sensitivity is upscaled by steering kernel regression method, so that the high resolution coil sensitivity can be obtained directly.

IV. EXPERIMENTAL RESULTS

A. *Experiment*

The proposed nonlinear coil sensitivity estimation method was applied to in vivo brain imaging experiment and compared with standard linear method to demonstrate its feasibility. The images acquired by

The in vivo anatomical brain data were fully acquired using a 3T scanner (SIGNA EXCITE, GE healthcare) with an 8-channel head coil. A 3D inversion recovery fast spoiled gradient recalled (3D IRfSPGR) sequence was used to acquire the axial brain images from a healthy volunteer. The parameters of the IRfSPGR sequence were: TR = 6.052 ms, TE = 2.844 ms, flip angle = 20°, slice thickness = 3 mm with zero slice gap, slice number = 20, FOV = 240 mm×240 mm, and the acquisition matrix = 256×256. The low resolution coil sensitivity data were acquired in a separate scan with the matrix size of 32×32.

The fully sampled k-space data were down-sampled to simulate different acceleration factors. The sum-of-squares image which was obtained using the fully sampled data was used as a gold standard for comparison. For linear reconstruction, the widely-used local polynomial fitting algorithm was used [5].

B. *Results*

Fig. 3 compares the coil sensitivity maps estimated by different methods. The 32×32 low resolution exhibits obvious mosaic effect. Meanwhile, there are also visible Gibbs ringing artifacts (the 1st row of Fig. 3).The coil sensitivity maps given by linear estimation method showed considerable Gibbs ringing artifacts (indicated by the black arrow in the 2nd row of Fig. 3). In comparison, the coil sensitivity maps estimated by the proposed nonlinear method effectively removed these Gibbs ringing artifact, showing a very smoothing result.

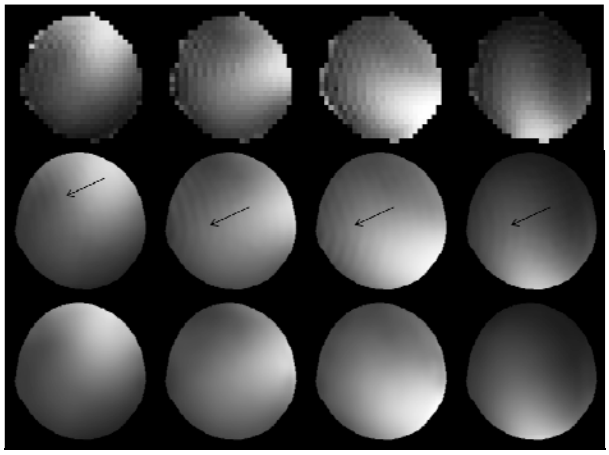

Figure 3. Coil sensitivity maps estimated by different methods. The 1st row shows 32×32 low resolution coil sensitivty; the 2nd row shows coil sensitivity estimated by standard linear method; the 3rd row shows coil sensitivity estimated by the proposed nonlinear method.

SENSE reconstruction results with coil sensitivity estimated by both linear and nonlinear method are compared in Fig. 4 for different reduction factors. Images reconstructed with linear coil sensitivity estimates (the 1st row of Fig. 4) show an overall higher noise level than that with nonlinear coil sensitivity estimates (the 2nd row of Fig. 4). As the reduction factor goes higher, images reconstructed with both methods exhibit an increasing noise level due to the ill-posedness of the SENSE reconstruction.

Fig. 5 compares the difference maps between images reconstructed with different coil sensitivity estimates and the sum-of-squares image for different reduction factors. For reduction factor 2, the result image based on linear coil sensitivity method shows visible residual aliasing artifact (as pointed to by the arrow in Fig. 5). For reduction factor 3, the image obtained by SENSE and linear coil sensitivity method shows obvious residual aliasing artifact. When the reduction factor is as high as 4, the reconstructed image using linear coil sensitivity estimate showed ringing-like noise as well as intensive residual aliasing artifact. In contrast, images reconstructed with nonlinear coil sensitivity estimates showed lower noise level and residual aliasing artifact level.

Tab. 1 summarizes the root mean square error (RMSE) of all experiment results. The image reconstruction with nonlinear coil sensitivity estimate shows the less RMSE for all tested reduction factors.

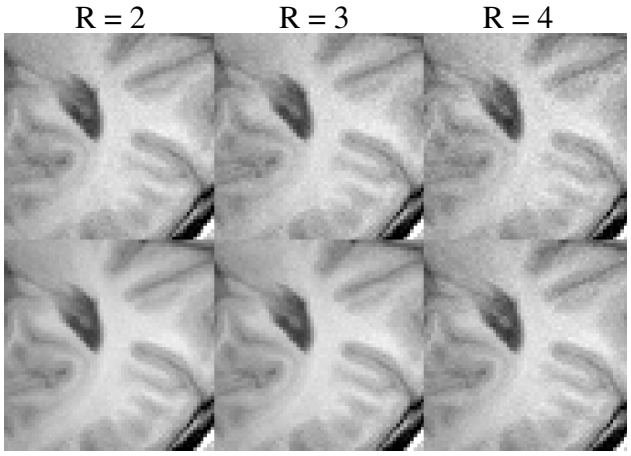

Figure 4. Zoomed-in part of SENSE reconstruction results using linear and nonlinear coil sensitivity estimates for different reduction factors. The 1st row shows SENSE reconstructed images using coil sensitivity estimated by standard linear method; the 2nd row shows SENSE reconstructed images using coil sensitivity estimated by the proposed nonlinear method.

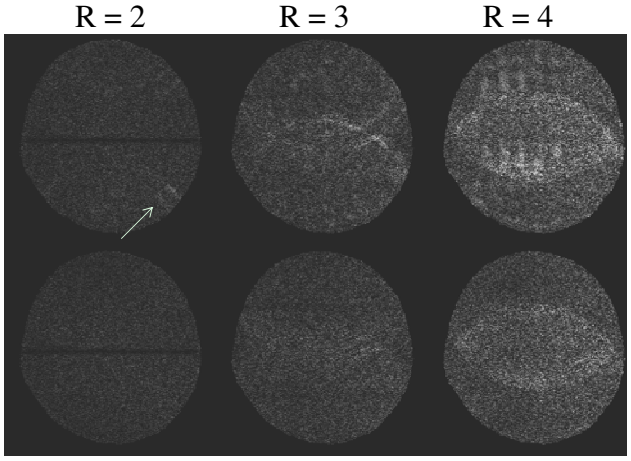

Figure 5. Difference maps of SENSE reconstruction results using linear and nonlinear coil sensitivity estimates for reduction factor 2, 3 and 4. The 1st row shows difference images for linear coil sensitivity estimation; the 2nd row shows difference images for the proposed nonlinear method.

TABLE I. RMSE OF IMAGES RECONSTRUCTED WITH LINEAR AND NONLINEAR COIL SENSITIVITY ESTIMATES

	R=2	**R=3**	**R=4**
Linear	0.59	1.08	2.01
Nonlinear	0.53	0.88	1.53

V. CONCLUSION

A new nonlinear coil sensitivity estimation method was proposed to improve the accuracy of coil sensitivity. The proposed method suppresses Gibbs ringing and reduces resolution loss effect in current linear method by utilizing nonlinear image upscaling technique that is based on data-adaptive steering kernel regression method. The in vivo experiments demonstrate that the proposed method can effectively improve the accuracy of coil sensitivity estimation, which reduces both the residual aliasing and noise power of SENSE reconstruction results in presence of poor resolution of coil sensitivity data.

REFERENCES

[1] D. K. Sodickson and W. J. Manning, "Simultaneous acquisition of spatial harmonics (SMASH): Fast imaging with radiofrequency coil arrays," *Magn Reson Med,* vol. 38, pp. 591-603, 1997.

[2] M. A. Griswold, P. M. Jakob, R. M. Heidemann, M. Nittka, V. Jellus, J. Wang, B. Kiefer, and A. Haase, "Generalized Autocalibrating Partially Parallel Acquisitions (GRAPPA)," *Magnetic Resonance in Medicine,* vol. 47, pp. 1202-1210, 2002.

[3] Yeh EN, McKenzie CA, Ohliger MA, and S. DK, "Parallel magnetic resonance imaging with adaptive radius in k-space (PARS): Constrained image reconstruction using k-space locality in radiofrequency coil encoded data," *Magnetic Resonance in Medicine,* vol. 53, pp. 1383-1392, 2005.

[4] C. Liu, R. Bammer, and M. E. Moseley, "Parallel imaging reconstruction for arbitrary trajectories using k-space sparse matrices (kSPA)," *Magn Reson Med,* vol. 58, pp. 1171-81, 2007.

[5] K. Pruessmann, M. Weiger, M. B. Scheidegger, and P. Boesiger, "SENSE: Sensitivity encoding for fast MRI," *Magnetic Resonance in Medicine,* vol. 42, pp. 952-962, 1999.

[6] M. A. Griswold, P. M. Jakob, M. Nittka, J. W. Goldfarb, and A. Haase, "Partially parallel imaging with localized sensitivities(PILS)," *Magnetic Resonance in Medicine,* vol. 44, pp. 602-609, 2000.

[7] W. E. Kyriakos, L. P. Panych, D. F. Kacher, C. F. Westin, S. M. Bao, R. V. Mulkern, and F. A. Jolesz, "Sensitivity profiles from an array of coils for encoding and reconstruction in parallel(SPACE RIP)," *Magnetic Resonance in Medicine,* vol. 44, pp. 301-308, 2000.

[8] L. Ying and J. Sheng, "Joint image reconstruction and sensitivity estimation in SENSE (JSENSE)," *Magnetic Resonance in Medicine,* vol. 57, pp. 1196-1202, 2007.

[9] F. H. Lin, Y. J. Chen, J. W. Belliveau, and L. L. Wald, "A wavelet‐based approximation of surface coil sensitivity profiles for correction of image intensity inhomogeneity and parallel imaging reconstruction," *Human brain mapping,* vol. 19, pp. 96-111, 2003.

[10] Charles A. McKenzie, Ernest N. Yeh, Michael A. Ohliger, Mark D. Price, and D. K. Sodickson, "Self-calibrating parallel imaging with automatic coil sensitivity extraction," *Magnetic Resonance in Medicine,* vol. 47, pp. 529-538, 2002.

[11] M. A. Griswold, F. Breuer, M. Blaimer, S. Kannengiesser, R. M. Heidemann, M. Mueller, M. Nittka, V. Jellus, B. Kiefer, and P. M. Jakob, "Autocalibrated coil sensitivity estimation for parallel imaging," *NMR in Biomedicine,* vol. 19, pp. 316-324, 2006.

[12] J. Zhang, C. Liu, and M. E. Moseley, "Parallel reconstruction using null operations," *Magnetic Resonance in Medicine,* vol. 66, pp. 1241-1253, 2011.

[13] M. Lustig and J. M. Pauly, "SPIRiT: Iterative self‐consistent parallel imaging reconstruction from arbitrary k‐space," *Magnetic Resonance in Medicine,* vol. 64, pp. 457-471, 2010.

[14] H. Takeda, S. Farsiu, and P. Milanfar, "Kernel Regression for Image Processing and Reconstruction," *IEEE Transactions on Image Processing,* vol. 16, pp. 349-366, 2007.

[15] A. Belahmidi and F. Guichard, "A partial differential equation approach to image zoom," 2004, pp. 649-652.

[16] A. Chambolle, "An algorithm for total variation minimization and applications," *Journal of Mathematical Imaging and Vision,* vol. 20, pp. 89-97, 2004.

[17] H. Takeda, S. Farsiu, and P. Milanfar, "Deblurring using regularized locally adaptive kernel regression," *Image Processing, IEEE Transactions on,* vol. 17, pp. 550-563, 2008.